Video Article

Stereotactic Atlas-Guided Laser Capture Microdissection of Brain Regions Affected by Traumatic Injury

Harris A. Weisz*[1], Deborah R. Boone*[1], Stacy L. Sell[1], Helen L. Hellmich[1]

[1]Department of Anesthesiology, University of Texas Medical Branch

*These authors contributed equally

Correspondence to: Helen L. Hellmich at hhellmic@utmb.edu

Abstract

The ability to isolate specific brain regions of interest can be impeded in tissue disassociation techniques that do not preserve their spatial distribution. Such techniques also potentially skew gene expression analysis because the process itself can alter expression patterns in individual cells. Here we describe a laser capture microdissection (LCM) method to selectively collect specific brain regions affected by traumatic brain injury (TBI) by using a modified Nissl (cresyl violet) staining protocol and the guidance of a rat brain atlas. LCM provides access to brain regions in their native positions and the ability to use anatomical landmarks for identification of each specific region. To this end, LCM has been used previously to examine brain region specific gene expression in TBI. This protocol allows examination of TBI-induced alterations in gene and microRNA expression in distinct brain areas within the same animal. The principles of this protocol can be amended and applied to a wide range of studies examining genomic expression in other disease and/or animal models.

Video Link

The video component of this article can be found at https://www.jove.com/video/56134/

Introduction

The mammalian brain is remarkably complex and heterogeneous with hundreds to thousands of cell types[1]. Indeed, human studies have shown that in regions such as the frontal cortex, structural and functional differences in white and grey matter are reflected in distinct and divergent transcriptional profiles[2]. Brain heterogeneity has been a major obstacle to interpret gene expression data and in the field of brain injury. This ambiguity in preclinical studies has subsequently led to hundreds of failed clinical trials of treatments for brain injury[3].

We use laser capture microdissection (LCM) methods to study traumatic brain injury (TBI)-induced gene dysregulation in the rat brain[4], focusing on the hippocampus, a brain region that is essential for learning and memory[5]. The ability to laser capture and analyze gene expression in both dying and surviving neurons gives us a greater understanding of the role of stochasticity in gene expression in determining the outcome (neuronal survival) after TBI[6]. LCM techniques have also proven useful for exploring the effects of TBI on hippocampal neurons when comparing young and aging mice[7] or rats[8].

In recent studies, we examined other regions of the rat brain adversely impacted by TBI, with a focus on areas in rats and in human TBI patients that are associated with executive function (*i.e.* frontal cortex[9]) and TBI comorbidities; these comorbidities include depression (*i.e.* nucleus accumbens[10]) and circadian rhythm disorders (suprachiasmatic nucleus[11]). In previous studies, Huusko and Pitkanen[12] and Drexel *et al.*[13] used LCM to examine gene expression in the thalamus and hypothalamus. Our study builds upon these prior observations and includes four other brain regions. To study the region-specific molecular changes induced after TBI, it was necessary to gain expertise in identifying and obtaining cell types in these regions using an LCM system. The UV-cutting and infrared (IR) lasers allow for precise microdissection of desired brain regions. Here, we describe how we use this LCM system, guided by stereotaxic coordinates in the rat brain atlas[14], to identify and laser capture four rat brain regions that are differentially affected by the experimental fluid-percussion brain injury method[4].

Protocol

NOTE: All animal experiments are approved by the Institutional Animal Care and Use Committee of the University of Texas Medical Branch, Galveston, Texas as directed by the National Institutes of Health Guide for the Care and Use of Laboratory Animals (8th Edition, National Research Council).

1. Tissue Collection, Region Identification, and Sectioning

1. Subject adult, male, Sprague-Dawley Rats, approximately six weeks old and 250 - 300 g, to experimental fluid percussion injury, as described in Shimamura et al.[4].
2. Twenty-four hours after experimental TBI, humanely euthanize the animals by placing them in a chamber with an isoflurane concentration of 4% until deeply anesthetized. Ensure death by decapitation, excise the brains, and immediately freeze in powdered dry-ice. Store frozen brains in a -80 °C freezer until sectioning.
3. Prior to any LCM procedure that includes transcriptional analysis, clean all surfaces with RNase eliminating detergent to mitigate the risk for contamination and RNA degradation.
   NOTE: This cleaning includes the area used for staining, the cryostat where tissue is sectioned, and the area around the LCM device.
4. Retrieve the brain tissue from storage and place into a cryostat cooled to -20 °C. Allow the brain to equilibrate to the temperature of the cryostat chamber for ~10 min.
5. Place the brain ventral side up on a gauze sheet on top of the cryostat stage. With a clean, RNase-free razor blade, cut off the posterior portion just rostral to the cerebellum (can be saved or discarded) and the portion just anterior to the optic chiasm (och).
6. Place a small amount of optimal cutting temperature (OCT) medium into two separate cryomolds. Place the brain (containing the frontal association cortex (FrA) and nucleus accumbens core (AcbC)) into the cryomolds anterior side down. Add sufficient OCT medium to cover the tissue.
   1. Repeat this step with the brain tissue containing the hippocampus (Hp) and suprachiasmatic nucleus (SCN).
   2. Allow the OCT medium to freeze completely for ~20 min in the cryostat.
7. Once the tissue and OCT medium are completely frozen, squeeze a small amount of OCT onto a mounting head and press the frozen cryomolds containing the tissue onto the mounting head. Allow the OCT to freeze completely so that the mold containing the tissue is securely attached to the head.
8. Secure the head attachment to the sectioning mount and tighten the screw. Adjust the cutting angle in relation to the cryostat blade with the adjustment levers to ensure sections are cut evenly.
9. Set the section thickness to 30 µm. When sectioning the tissue block containing the FrA and AcbC, first begin sectioning until cerebral cortex is apparent and then start collecting.
10. Referring to the Rat Brain Atlas[12], section and collect brain sections by gently placing room-temperature polyethylene napthalate (PEN) membrane slides on top of the sectioned tissue for the FrA until the secondary motor cortex (M2) is reached at Bregma 5.16 mm.
    1. Visually ensure adherence to slide by inspecting if tissue and OCT are completely melted onto slide. Store all slides with tissue sections in the cryostat until staining.
11. Continue sectioning until the anterior commissure (aca) becomes visible and unites into one complete commissure underneath the now apparent lateral ventricles (LV) at Bregma 1.80 mm.
12. Collect sections until the LVs appear to connect with the aca at Bregma 0.84 mm.
13. Once sectioning for the FrA and AcbC has been completed, remove the mounted tissue block, and replace with the block containing HP and SCN.
14. Section until the och is flattened at Bregma -0.48 mm, when the third ventricle (3V) becomes apparent.
15. Collect sections for the SCN from this point until Bregma -0.72 mm, when the supraoptic decussation (sox) begins.
    NOTE: It may be necessary to collect more tissue sections throughout the och as the SCN is easily passed over.
16. For HP collection, section until the horns of granule cell layer dentate gyrus (GrDG) are visibly apparent at Bregma -3.00 mm.
17. Collect sections until the hippocampal CA subfields are fused in the coronal sections at Bregma -4.78 mm. This detail allows for complete collection of the hippocampus under the craniotomy and injury site.
    NOTE: As demonstrated in previous publications from this lab, most injured cells will be apparent within this range and it is appropriate for gene or microRNA expression analysis.

2. Staining Protocol

1. Prior to staining, wash all dishware and the staining area in a chemical fume hood with RNase-eliminating detergent. This preparation mitigates the risk of RNA degradation due to contamination.
2. Prepare all staining reagents and solutions in nuclease free water.
3. Take a rack of slides stored in the cryostat and place in the fume hood. Allow slides to warm for 30 s. Place them into staining solutions (prepared with nuclease free water) as follows: 75% EtOH for 1 min, nuclease free water for 1 min, 1% cresyl violet for 1 min, nuclease free water for 30 s, nuclease free water for 30 s, 95% EtOH for 30 s, 100% EtOH for 30 s, xylene for 3 min, and xylene for 3 min.
4. Allow the rack to air-dry for no more than 10 min at room temperature in the fume hood. Alternatively, place racks into an Rnase-free vacuum desiccator for quicker drying. Once dried, proceed immediately to LCM.

3. Stereotactic Atlas Guided Laser Capture Microdissection with the LCM System

1. Prior to beginning any LCM procedure for RNA analysis, wipe down the collection area and the area around the device with RNase-eliminating detergent and 100% EtOH.
2. Flip the power switch on the IR laser generating unit before turning on microscope base, and allow the system to initialize before software is started from the desktop.
   NOTE: If not completed in this order, the software will not recognize the microscope.
3. Once the software has booted and run through its initializing steps, press the "Present Stage" button in the software "Setup Panel." The modular stage will move into position where LCM Macro Caps and slides can be loaded and off-loaded.
4. Place the PEN membrane slides into the holders (up to three at a time) with the frosted edge facing rightward.
   NOTE: If placed in the holder in the wrong orientation, the software may not be able to properly recognize the desired IR or UV cutting area.

5. Click the "Mem" checkbox in the "Cap and Slide Handling Area" next to the respective slide (*i.e.*, A, B, or C). This step denotes if the slide is a membrane glass slide. Then click on the desired slide to be captured first.
6. To make the camera take a tiled image for tissue location and orientation for cap placements, select "Image" on the Toolbar and select "Acquire Overview."
   NOTE: If the user is familiar with the tissue being collected, this step can be omitted by using the manual scroll ball to position the "Region Center" for collection.
7. Place the cursor over the area on the tiled image (or relative location without tiled image), right click and select "Place Cap at Region Center." The software will automatically place a cap over the selected position.
8. Select a location.
   NOTE: To ensure that the IR laser is properly aligned and will pick up only areas where spots are laid by the software it must be located before proceeding.
   1. Move to an area within the cap where no tissue is present. Click "i" in the "Microdissect Tools Pane" and select the "IR Locate" tab. From the Pane, fire an IR test shot to assess where the IR laser is firing and the size of the spot.
   2. With the cursor, right click in the middle of IR spot and select "Located IR Spot."
      NOTE: Size and intensity of the IR beam can be changed by manually altering the "Power, Diameter, or Duration" under each spot size designator or by moving the sliding scale at the bottom of the dialog box. Several test shots may need to be fired to ensure proper spot size. The IR laser must be re-located each time the position of the cap changes or slides are switched.
   3. For UV cutting, locate the UV laser by selecting the "UV Locate" tab in the dialog box.
      NOTE: Because the UV laser and the IR laser move in unison, there is no need to continually re-locate the UV laser each time the position is changed.

9. Choose the "Freehand Drawing" option in the "Select Tools Pane". Using a touchscreen stylus, draw around the perimeter of the region of interest while making sure not to lose contact between the touchscreen and the stylus head. Make sure to connect the beginning and end-points together.
   NOTE: IR spots will be laid down automatically through the software but the user may choose to lay down additional spots to ensure the tissue is adhered to the cap after UV cutting has been performed.
10. For FrA collection, perform a gross laser capture of cortical tissue up to when the M2 cortex appears at Bregma 5.16 mm.
    NOTE: This detail can be amended such that only specific portions of the FrA or specific cell types are collected.
11. For AcbC collection, laser capture an area close in proximity to the aca.
    The core and shell of the AcbC perform different functions and are physiologically unique. Thus it is important to follow the brain atlas as close as possible. It is recommended to collect from no further past bregma 0.84 mm, as the two subregions become too closely associated with each other.
12. For Hp collection, laser capture the CA 1, 2, and 3 hippocampal subfields starting at Bregma 3.00 mm and using the completely formed GrDG as a physical landmark for morphological identification.
    NOTE: For the purposes of this study, do not collect past Bregma -4.78 mm, which can be visually demarcated as the point when the Hp subfields are fused and point ventrally. This area was chosen as most injured neurons can be discovered directly under the injury site[6].
13. For SCN collection, first visually identify the densely packed nuclei that sit dorsal to the och and then collect.
14. After collection of regions (listed above), move LCM Macro Caps to the "QC position" and inspect for complete tissue adherence by visually ensuring UV cut tissue is attached to the membrane. Quickly place the cap ontoan RNase-free 0.5 mL thin walled reaction tube containing 100 μL of cell lysis buffer.
15. Vortex samples briefly to ensure complete lysis and store at -80 °C. At this point, LCM can be paused and samples stored until used for downstream genomic analysis[6].

Representative Results

The schematic presented in **Figure 1** illustrates the overall workflow of atlas guided LCM of specific brain regions and potential downstream analysis applications. This study focused on four brain regions relevant to TBI pathophysiology and to the development of comorbidities: FrA, AcbC, SCN, and Hp. A limitation present in LCM of specific brain regions is that anatomical locations are often obscured by a lack of defined boundaries, as can be seen in **Figure 2 (A, D, G, J)**. The use of a brain atlas to guide sectioning and laser capture of specific regions reduces the possibility of sample contamination with brain regions other than the target. When care is taken to follow tissue landmarks, both during sectioning and after Nissl-staining, LCM technology can provide a highly consistent means of acquiring discrete populations of cells, nuclei, or regions[15]. The long-term goals of these studies are to identify genes and microRNAs that can potentially serve as surrogate, non-invasive biomarkers of brain region specific injury. The first step in this biomarker development pipeline is the characterization of tissue-specific transcriptional changes after experimental TBI. These data can then be correlated with injury-induced changes in circulating biofluids.

The presented procedures were optimized to mitigate risk of RNA degradation in order to allow RNA analysis via reverse transcription of total LCM RNA before quantitative real-time PCR (RT-qPCR). Total RNA (including small and large RNA species) was isolated using a column-based isolation method on tissue that was laser-captured from individual brain regions. To assess RNA integrity, quality, and quantity after isolation procedures, RNA samples were briefly denatured at 70 °C and run on an RNA analyzer. Qualitative measurements included analyzing peak amplitudes of the 18s and 28s rRNA bands **(Figure 3)**, which can be representative of overall degradation, and using the "RNA Integrity Number" (RIN). If using careful RNase-free techniques, RNA isolated from LCM samples typically results in RINs that range from 6-8. A lower RIN can imply poor RNA quality and can potentially decrease the accuracy of gene and microRNA expression analysis. Conversely, a higher RIN can improve confidence in the validity of results generated from RNA analysis.

RT-qPCR was performed using primer/probe sets for individual genes and microRNAs (**Figure 4**). Approximately 1 ng of total RNA was reverse-transcribed into cDNA and pre-amplified before qPCR was performed according to manufacturer's protocol. Injury-related genes assessed in this study included *BCL2 Associated X, Apoptosis Regulator* (*Bax*), *B-Cell CLL/Lymphoma 2* (*Bcl-2*), *Caspase 3, Apoptosis-Related Cysteine Peptidase* (*Casp3*), *Brain Derived Neurotrophic Factor* (*Bdnf*), and *CAMP Responsive Element Binding Protein 1* (*Creb*). MiR-15b was selected because it has been shown to be altered after experimental TBI in individual dying neurons. It also has experimentally validated and bioinformatically predicted gene targets with pro-survival functions (unpublished data). Normalized fold-change ratios were calculated by $\Delta\Delta$Ct method comparing gene and microRNA expression levels in TBI animals and naïve controls, with normalization to an endogenous gene (*Gapdh*) or small RNA (*U6*), respectively. A fold-change above 1 indicates an overall upregulation in that gene or microRNA, and conversely, a fold change lower than 1 indicates a downregulation. Statistical analysis showed significant changes in gene expression between TBI and naïve control ($p \leq 0.05$) that were brain region dependent. No significant changes in miR-15b expression were detected between TBI and naïve control, but there were trends towards higher and lower expression in a brain region dependent fashion. These data suggest that further optimization is necessary to assess changes in microRNA expression. It is also possible the sample size was too small to gain statistical significance, in part due to inherent variability in expression. Future studies will include sham-operated animals to ensure that gene and microRNA expression changes are attributed to TBI and not due to the surgical preparation.

Figure 1. Workflow of Atlas-guided LCM for Downstream Genomic Analysis. (A-F) Procedures from animal preparation to downstream qPCR analysis: **(A)** Adult, male Sprague Dawley rats (~6 weeks of age and weighing 300 g) are anesthetized, subjected to fluid percussion TBI, and humanely euthanized 24 h after injury. **(B)** Serial sections (30 μm) of fresh frozen brains are based on coordinates of specific brain regions (FrA, AcbC, Hp, SCN) from Paxinos and Watson's The Rat Brain atlas. **(C)** Sections are fixed, Nissl-stained (1% Cresyl Violet), dehydrated, and air dried. **(D)**. LCM performed on identified brain regions with an LCM System. **(E)** LCM Macro Caps transferred onto an RNase-free 0.5 mL tube with 100 μL of cell lysis buffer and stored at -80 ºC until RNA isolation for downstream genomic analysis. RNA can then be reverse-transcribed for gene or microRNA RT-qPCR analysis to examine differential expression of molecular target(s) after TBI and/or between brain regions of interest **(F)**. Please click here to view a larger version of this figure.

Figure 2. LCM of TBI Affected Brain Regions. Representative images of tissue sections collected from the ipsilateral side of injury site with IR and UV laser functions on the LCM system **(A-I)**. Tissue was sectioned on a cryostat (30 µm) and collected on PEN membrane slides. Sections were then fixed, Nissl-stained with cresyl violet (1%), and dehydrated to identify specific brain regions based on anatomical landmarks referenced in Paxinos and Watson's The Rat Brain Atlas. **(A-C)** An area of the frontal association cortex (FrA) **(D-F)** Components of the CA1, CA2, and CA3 pyramidal layers of the hippocampus (Hp) located next to the fully formed horns of the granule layer of the dentate gyrus (GrDG). **(G-I)** An area of the nucleus accumbens core (AcbC) proximal and rostral to the anterior commissure (aca). **(J-K)** Suprachiasmatic nucleus (SCN) rostral to the supraoptic chiasm (och). Please click here to view a larger version of this figure.
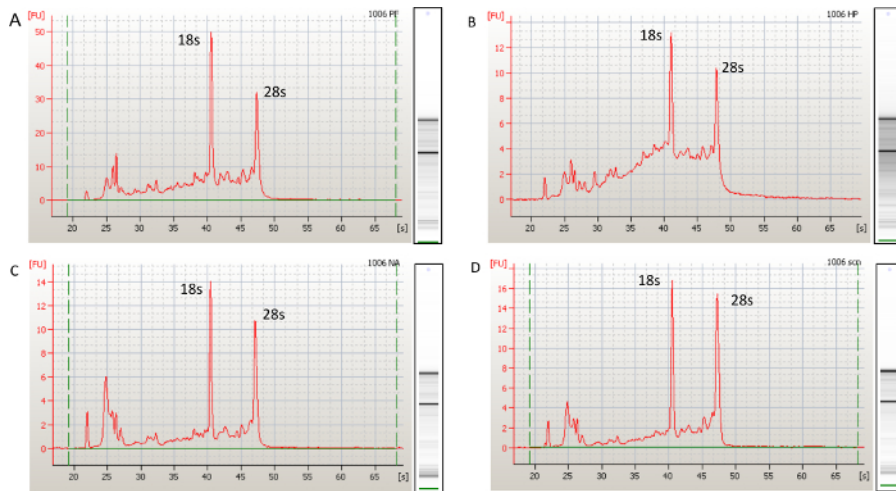
Figure 3. Representative Scans of RNA Quality. Representative electropherograms and associated gel images of RNA derived from LCM collected tissue **(A-D)**. Electropherograms and associated gel images show intact RNA based on appearance of 18s and 28s rRNA peaks and gel bands. This RNA is suitable for all downstream applications, including genomic and proteomic analyses. **(A)** Frontal association cortex (FrA) RNA. RIN 6.1. **(B)** Hippocampus (Hp) RNA. RIN 4.4. **(C)** Nucleus accumbens core (AcbC) RNA. RIN 7.3. **(D)** Suprachiasmatic nucleus (SCN) RNA. RIN 7.6. Please click here to view a larger version of this figure.
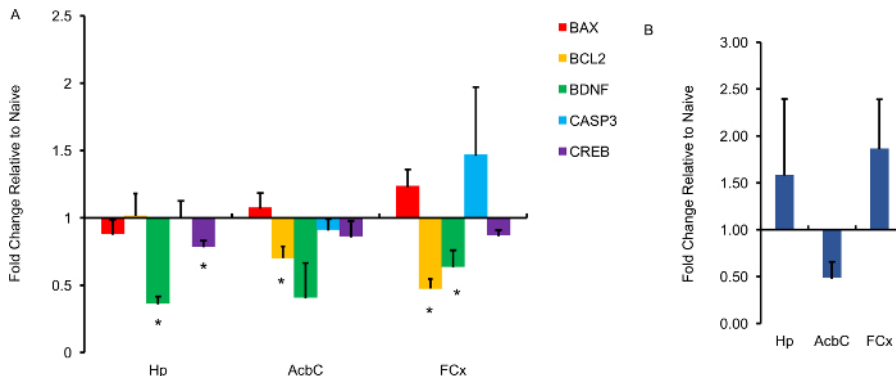
Figure 4. Downstream Analysis of Brain Region-specific Gene and MicroRNA Expression *via* RT-qPCR. Individual RT-qPCR for genes of interest (*Bax, Bcl-2, Bdnf, Casp3, Creb*) and microRNA of interest (miR-15b) was performed on laser captured brain regions after TBI (Hp and AcbC n= 5, FrA n= 4) and compared to uninjured naïve animals (n= 4). Analysis of genes related to TBI pathogenesis was performed for Hp, AcbC, FCx. Data is presented as normalized fold change ratios compared to naïve control brain regions (Unpaired t test with Welch's Correction ± SEM; * $p \le 0.05$) **(A)**. Differential expression of miR-15b in different brain regions is presented as normalized fold changes compared to naïve control (± SEM) **(B)**. Data from SCN (n=2) not included. Please click here to view a larger version of this figure.

Discussion

For molecular studies of the mammalian brain, LCM has become an essential technique. This article demonstrates that using the combination of the IR and UV cutting lasers in the LCM system can capture genomic changes in any region of the mammalian brain. These regions include those identifiable with conventional LCM-compatible stains, such as cresyl violet or hematoxylin and eosin. The speed of the laser-capture process and ability to perform LCM on thicker 30 µm sections on PEN membrane slides allows to not only obtain sufficient quantities of cell samples, but also to isolate RNA from LCM samples of a suitable quality for all types of downstream genomic analysis; these analyses include microarrays[16], PCR arrays[17], and quantitative real-time PCR[18].

Our data provide a rationale for studies which utilize LCM tissue. We find that miR-15b is upregulated in the hippocampus and cortex (**Figure 4**) but downregulated in the nucleus accumbens and may be biologically relevant to the understanding of differential effects of TBI in the brain. A previous study suggested that increases in cortical neuronal vulnerability to injury result from overexpression of several miRNAs that negatively regulate pro-survival genes, such as Bcl-2[19]. Target scan analysis shows Bcl-2 is also regulated by miR-15b; thus, our data suggest a mechanistic explanation for why specific regions of the brain (*i.e.*, FCx) may be selectively vulnerable to TBI. It is important to remember most genes are regulated by multiple miRNAs and correlating changes in any one miRNA to a specific target gene is difficult. Moreover, these data indicate that certain changes in gene and microRNA expression may be used as biomarkers of region-specific brain damage. Indeed, we are currently using these data in studies of how new neuroprotective drug compounds with antidepressant properties can differentially affect gene and microRNA expression in brain regions linked to neuropsychiatric disorders. One limitation of our study is that during the multiple steps of slide preparation processes for LCM, RNA integrity may become compromised. This protocol describes the necessary steps to mitigate the risk of RNA degradation. Another limitation is the relatively small sample size used for statistical calculation. In future studies, increasing sample size should lessen the effects of gene and miRNA expression variations among individual animals.

The benefit of LCM is realized in translational genomic studies using animal models of human disease and diseased tissues[20,21,22,23]. Without the ability to capture specific cell populations, the transcriptional profiles of different brain regions would be an unknowable and undecipherable mix of many cell types. Using LCM methods in brain injury studies has led to current efforts to delineate brain region specific biomarkers and to understand how they correlate with circulating biomarkers of TBI.

Disclosures

The authors have nothing to disclose.

Acknowledgements

References

1. Bota, M., Dong, H.W., & Swanson, L.W. From gene networks to brain networks. *Nat. Neurosci.* **6** (8), 795-799, (2003).
2. Mills, J.D. *et al.* Unique transcriptome patterns of the white and grey matter corroborate structural and functional heterogeneity in the human frontal lobe. *PLoS One.* **8** (10), e78480 (2013).
3. Doppenberg, E.M., Choi, S.C., & Bullock, R. Clinical trials in traumatic brain injury: lessons for the future. *J Neurosurg Anesthesiol.* **16** (1), 87-94, (2004).
4. Shimamura, M., Garcia, J.M., Prough, D.S., & Hellmich, H.L. Laser capture microdissection and analysis of amplified antisense RNA from distinct cell populations of the young and aged rat brain: effect of traumatic brain injury on hippocampal gene expression. *Mol Brain Res.* **17** (1), 47-61, (2004).
5. Bast, T. Toward an integrative perspective on hippocampal function: from the rapid encoding of experience to adaptive behavior. *Rev Neurosci.* **18** (3-4), 253-281, (2007).
6. Rojo, D.R. *et al.* Influence of stochastic gene expression on the cell survival rheostat after traumatic brain injury. *PLoS.One.* **6** (8), e23111, (2011).
7. Shah, S.A., Prough, D.S., Garcia, J.M., DeWitt, D.S., & Hellmich, H.L. Molecular correlates of age-specific responses to traumatic brain injury in mice. *Exp Gerontol.* 2006 Nov; **41**(11): 1201-5. Epub 2006 Sep 15 (2006).
8. Shearer, J. *et al.* Stochastic fluctuations in gene expression in aging hippocampal neurons could be exacerbated by traumatic brain injury. *Aging Clin.Exp.Res.* (2015).
9. Caeyenberghs, K. *et al.* Altered structural networks and executive deficits in traumatic brain injury patients. *Brain Struct.Funct.* **219** (1), 193-209 (2014).
10. Bewernick, B.H., Kayser, S., Sturm, V., & Schlaepfer, T.E. Long-term effects of nucleus accumbens deep brain stimulation in treatment-resistant depression: evidence for sustained efficacy. *Neuropsychopharmacology.* **37** (9), 1975-1985, (2012).
11. Karatsoreos, I.N. Effects of Circadian Disruption on Mental and Physical Health. *Curr.Neurol.Neurosci Rep.* (2012).
12. Drexel, M., Puhakka, N., Kirchmair, E., Hörtnagl, H., Pitkänen, A., & Sperk, G. Expression of GABA receptor subunits in the hippocampus and thalamus after experimental traumatic brain injury. *Neuropharmacology.* **88**, 122-133, (2015).
13. Huusko, N., Pitkanen, A. Parvalbumin immunoreactivity and expression of GABAA receptor subunits in the thalamus after experimental TBI. *Neuroscience.* **16** (267), 30-45, (2014).
14. Paxinos, G., & Watson, C. *The rat brain in stereotaxic coordinates.* 7th edn., Academic Press, (2013).
15. Boone, D.R., Sell, S.L., & Hellmich, H.L. Laser capture microdissection of enriched populations of neurons or single neurons for gene expression analysis after traumatic brain injury. *Journal of Visualized Experiments.* **74** (e50308), 1-7, (2012).
16. Hellmich, H.L. *et al.* Pathway analysis reveals common pro-survival mechanisms of metyrapone and carbenoxolone after traumatic brain injury. *PLoS.One.* **8** (1), e53230, (2013).
17. Boone, D.R. *et al.* Pathway-focused PCR array profiling of enriched populations of laser capture microdissected hippocampal cells after traumatic brain injury. *PLoS.One.* **10** (5), e0127287 (2015).
18. Boone, D.R. *et al.* Traumatic Brain Injury-induced Dysregulation of the Circadian Clock. *PLoS.One.* **7** (10), e46204, (2012).
19. Truettner, J.S., Motti, D., & Dietrich, W.D. MicroRNA overexpression increases cortical neuronal vulnerability to injury. *Brain Res.* **1533** 122-130, (2013).
20. Hellmich, H.L. *et al.* Traumatic brain injury and hemorrhagic hypotension suppress neuroprotective gene expression in injured hippocampal neurons. *Anesthesiology.* **102** (4), 806-814, (2005).
21. Ginsberg, S.D., Alldred, M.J., & Che, S. Gene expression levels assessed by CA1 pyramidal neuron and regional hippocampal dissections in Alzheimer's disease. *Neurobiol.Dis.* **45** (1), 99-107, (2012).
22. Elstner, M. *et al.* Expression analysis of dopaminergic neurons in Parkinson's disease and aging links transcriptional dysregulation of energy metabolism to cell death. *Acta Neuropathol.* **122** (1), 75-86, (2011).
23. Wang, S. *et al.* Improvement of tissue preparation for laser capture microdissection: application for cell type-specific miRNA expression profiling in colorectal tumors. *BMC.Genomics.* **11** 163, (2010).